Determination of PMMA Etch Rates Using VASE Modeling

V. Vazquez[1], Z. Kranefeld[1], J. H. McElearney[1], and T. E. Vandervelde*[1]
[1]Department of Electrical and Computer Engineering, Tufts University, Medford, MA, 02155

ABSTRACT

Variable angle spectroscopic ellipsometry (VASE) was used to determine the thicknesses of polymethyl methacrylate (PMMA) on Si before and after etching with two different etchants (CF_4 + O_2 and Argon). Once a complete optical model for a base PMMA on Si sample was created, it was applied to all etched samples to determine thicknesses. Despite some minor changes to the optical behavior of PMMA caused by the Ar etching, our ability to fit to observed interference peaks remained unaffected. This technique allows for nanometer accurate thickness measurements, which is an improvement from current thickness measurement methods such as stylus profilometry.

Keywords: VASE Modeling, PMMA, Metrology, IC Fabrication

1. INTRODUCTION

From creating micro prisms on glass substrates to fabricating smoother nanowires, gray-scale lithography allows for the creation of microstructures that can enhance the performance of power electronics and electronic circuitry [1-3]. The precision of these microstructures heavily depends on accurate etch rates of the resist and base substrate. Etch rates are most commonly determined by stylus profilometry, frequently used in finding thin-film thickness, erosion calculations, and determining surface roughness [4-6]. However, stylus profilometry is limited to sub-micron accuracy, making it unsuitable for nanometer scale devices such as nanowires and quantum dots [7-11]. This constraint makes it unfavorable for precise masks using gray-scale lithography, as well as determining etch selectivity. An accurate etch selectivity allows for finer control of nanostructures in desired materials. Variable angle spectroscopic ellipsometry (VASE) measurements allow for nanometer precision thicknesses of materials with known optical constants. Ellipsometry is effective for thin film measurements, especially when grown on a thick opaque material [12].

In this work, VASE was used to find the thicknesses of various polymethyl methacrylate (PMMA) on Si samples. VASE scans were performed before and after etching using multiple etchants and etch times. In advance of these measurements, scans of a bare Si wafer, and two PMMA films of known thickness, were taken to obtain the exact optical properties of our materials. VASE can potentially be exploited to get accurate thickness measurements for lithography processes, or in any processes that require nanometer accurate thickness measurements.

2. EXPERIMENTAL METHODS

Two four-inch Si wafers had 950PMMA [13] resist with 4% anisole spun on them, targeting a 200 nm and 400 nm PMMA film, with the approximate thicknesses based on spin speed curve charts. In preparation of etching, each 4-in Si wafer with PMMA was diced into 20 mm squares, with the center piece removed to keep the samples as similar as possible. Samples were etched by inductively coupled plasma reactive ion etch (ICP RIE) using either a CF_4 + O_2 or Ar gas on an Oxford PlasmaPro 100 Cobra 300. Samples with their etch recipes are shown in Table 1.

*tvanderv@ece.tufts.edu

Physics and Simulation of Optoelectronic Devices XXXII, edited by Bernd Witzigmann, Marek Osiński, Yasuhiko Arakawa, Proc. of SPIE Vol. 12880, 128800T
 · 0277-786X · doi: 10.1117/12.3002035

Table 1. Samples with their corresponding etch recipes.

Sample Name	Starting PMMA Film Thickness (nm)	Etchant	Etch Time (s)
A	207.0	CF_4+ O_2	20
B	207.0	Ar	20
C	207.0	CF_4+ O_2	25
D	207.0	Ar	30
E	207.0	Ar	45
F	207.0	Ar	60
G	415.6	CF_4+ O_2	30
H	415.6	Ar	30
I	415.6	CF_4+ O_2	30
J	415.6	CF_4+ O_2	60
K	415.6	Ar	60
L	415.6	CF_4+ O_2	90
M	415.6	Ar	90

When collecting VASE data of the samples, monochromatic light is split into a known combination s- and p- polarized light. This light reflects off the sample and the s- and p- polarized light is detected individually. The effective dielectric function of the sample changes how the light is reflected. Since s- and p-polarized light will reflect differently, the complex refractive index of the sample can be determined based on the normalized ratio of reflected p and s polarized light. This ratio is defined as ρ

$$\rho = \frac{E_{r,p}/E_{i,p}}{E_{r,s}/E_{i,s}} = \frac{r_p}{r_s} = \tan(\Psi)\, e^{i\Delta} \quad (1)$$

with tan (Ψ) being the ratio of the normalized amplitude of the reflected p- and s- polarized light, and Δ being the phase difference between them. This ratio can then be used to find the effective dielectric constant of the sample in the form ($\varepsilon = \varepsilon_1 + i\varepsilon_2$) with the equation [14]

$$\langle \varepsilon \rangle = \sin^2(\Phi) * \left[1 + \tan^2(\Phi) * \left(\frac{1-\rho}{1+\rho}\right)^2\right] \quad (2)$$

with ϕ being the angle of incidence. This effective dielectric function can then be used to find the effective complex refractive index given by

$$\langle \varepsilon \rangle = \langle \tilde{n} \rangle^2 \quad (3)$$

From the effective dielectric function, information about an individual layer can be extracted by building a layer-by-layer model and fitting the simulated data to the measured data. To find the optical constants of a desired layer, the thicknesses of all the layers, and the optical constants of every other layer must be known. The simulated data of the optical model can be changed to match the measured data by adjusting the refractive index of the unknown material layer of the sample. The layer of interest is built out of a series of oscillators, such as Gaussian and Tauc-Lorentz, which are adjusted until a sufficiently good fit to the measured data is achieved [15]. Alternatively, if the material's optical constants are known, the

thicknesses of that material can be found by adjusting the thickness value until the simulated spectra is sufficiently fitted to the measured spectra.

To find the thickness of the etched PMMA, the optical properties of both the Si and pre-etch PMMA of our samples needed to be known. Initial scans were taken of a bare, 0.5mm thick Si wafer, and of two PMMA films of known thicknesses. Existing optical models of Si [16] and PMMA [17] were used as starting points and adjusted to match the measured data from our samples. This baseline PMMA on Si optical model was used on all etched samples, with only PMMA thickness being adjusted to fit. The key fitting features were the interference peaks of the measured data since they are predominantly thickness dependent. Additionally, a Bruggeman Effective Medium Approximation (EMA) was applied to each model to improve the optical model fit to the measured data by accounting for the effect the surface might have on the sample's optical behavior. A Bruggeman EMA layer is a 50/50 mixture of the underlayer and void, which has been shown to assist in simulating surface oxides and roughness [18].

The optical properties of the PMMA layer were tailored to the measured data of the assumed ~200 nm sample until the simulated data more closely matched the measured data. Once the optical properties were as close as we could achieve, the layer thickness was allowed to vary around the assumed 200 nm. The resultant thickness of 207.0 nm ± 0.1 nm, has the fit shown in Fig.1. The measured data from the ~400 nm PMMA on Si sample was imported into the model and refit, which resulted in a thickness of 415.6 nm ± 0.1 nm. With the optical model of PMMA on Si verified, the measured data of all the etched samples were imported into the model and re-fit, with the thickness of the PMMA being the only changing variable.

VASE data was taken on a J.A. Woollam UV-VIS VASE over a wavelength range of 300 – 2000 nm in 5 nm steps. Scans were taken at several incidence angles (65, 70, and 75º). Since the location of the interference peaks are angle dependent, this gave additional features to fit against. Scans were performed on the diced chips and modeled using the WVASE software.

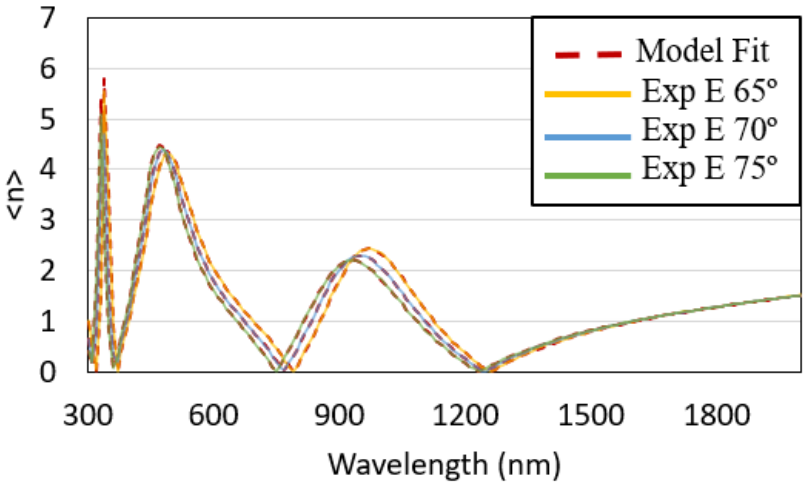

Fig. 1. ~200 nm PMMA on Si sample refractive index graph as a function of wavelength.

3. RESULTS

Both the amount of PMMA etched and etch rates were determined as a function of etch time. The modeled and measured spectra for PMMA after both $CF_4 + O_2$ and Ar etching are shown in Fig. 2b and 2c, respectively. The $CF_4 + O_2$ etched and pre-etched samples fit nearly identically. However, for the Ar etched samples, the refractive index of the PMMA had lower magnitude peaks from 200-500 nm than our model predicted, as seen in Fig. 2c. We attribute this change to either a roughening of the sample surface or some level of Ar ion implantation, though a more thorough investigation would be

required to say so with confidence. Despite this, as our fitting was based primarily on the location of these interference peaks, and not necessarily their magnitude, we still have confidence in the thickness measurements obtained.

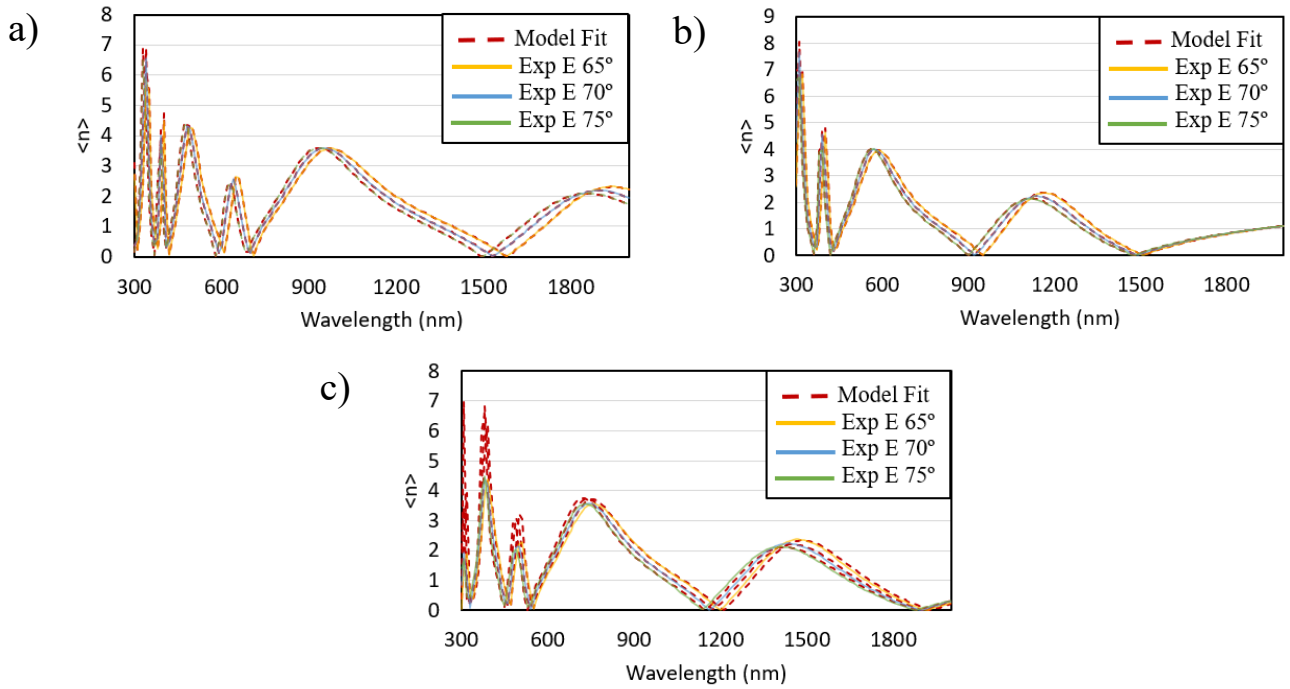

Fig 2. The refractive index of PMMA on Si a) pre-etch, b) post-etch with $CF_4 + O_2$ etchant, c) post-etch with Ar as an etchant

Building on the findings presented in Fig. 3, the consistent trendlines derived from both the amount of PMMA etched and etch rates provide valuable insights into the behavior of the etchants, highlighting their potential applications. Specifically, these trendlines allow for the estimation of an appropriate etch time to achieve a desired PMMA thickness, a key consideration for potential lithographic use, as shown in Fig. 3(left). Beyond demonstrating the validity of our technique, it was observed that the CF4 + O2 etchant removed the PMMA faster than the argon. The etch rates of both etchants decreased as etch time increased, as we would expect based on existing literature [19, 20].

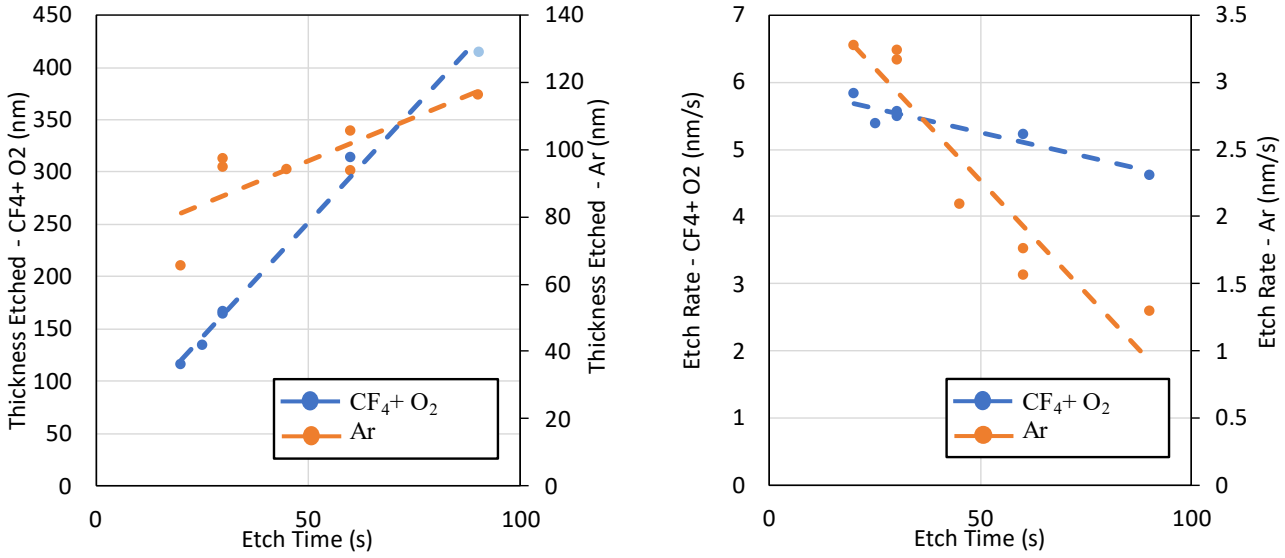

Fig 3. Calculated PMMA etched (left) and etch rates (right) from both the CF_4 + O_2 and Ar etchants as a function of the etch time. The trend lines are being used for a visual guide only and are not a linear fit.

4. CONCLUSION

We demonstrate a new method of etch rate measurements using VASE since it allows for the measurement of thin films with nanometer accuracy. The etch rates of PMMA were determined using two etchants (CF_4 + O_2 and Argon) and were shown to be inversely proportional to etch time. This is very useful when doing gray-scale lithography, where having an accurate measurement of the base resist allows for the creation of precise masks. Also, being able to get the etch rates from a specific etchant for a certain material would allow for more precise etching. The etch rates of multiple samples were calculated accurately using one finished optical model. Once a good understanding of a material's optical properties is established, VASE can be used to determine etch rates and thicknesses for a large number of samples very quickly. Ellipsometry is also line compatible, so it can be incorporated into production lines to ensure proper calibration.

5. ACKNOWLEDGEMENTS

This work is supported by the National Science Foundation (ECCS-2120568, as well as ECCS-2225641). This work was performed in part at the Harvard University Center for Nanoscale Systems (CNS); a member of the National Nanotechnology Coordinated Infrastructure Network (NNCI), which is supported by the National Science Foundation under NSF awards no. ECCS-2025158.

REFERENCES

[1] Waits, C.M., Morgan, B., Kastantin, M., Ghodssi, R., "Microfabrication of 3D silicon MEMS structures using gray-scale lithography and deep reactive ion etching", Sensors and Actuators A 119, 245–253 (2005)

[2] Gimkiewicz, C., Hagedorn, D., Jahns, J., Kley, E.B., Thoma, F., "Fabrication of microprisms for planar optical interconnections by use of analog gray-scale lithography with high-energy-beam–sensitive glass", APPLIED OPTICS, Vol. 38, No. 14, 2986–2990 (1999)

[3] Bolten, J., Wahlbrink, T., Schmidt, M., Gottlob, H., Kurz, H., "Implementation of electron beam grey scale lithography and proximity effect correction for silicon nanowire device fabrication", Microelectronic Engineering 88, 1910-1912 (2011)

[4] Iglesias, F., Aguilera, A., Padilla, A., Vizan, A., Diez, E., "Application of computer vision techniques to estimate surface roughness on wood-based sanded workpieces", Measurement 224, 113917, 1-17 (2023)

[5] Gyurkovics, M., Baumann, T., Carvalho, T.S., Assunção, C.M., Lussi, A., "In vitro evaluation of modified surface microhardness measurement, focus variation 3D microscopy and contact stylus profilometry to assess enamel surface loss after erosive–abrasive challenges", PLOS ONE, e0175027, 1-13 (2017)

[6] Pandurangarao, K., Ravi Kumar, V., "Preparation and characterization of nanocrystalline tungsten oxide thin films for electrochromic devices: Effect of deposition parameters", Materials Today: Proceedings 19, 2596-2603 (2019)

[7] Lim, J., Jeong, B.G., Park, M., Kim, J.K., Pietryga, J.M., Park, Y.S., Kilmov, V.I., Lee, C., lee, D.C., Bae, W.K., "Influence of Shell Thickness on the Performance of Light-Emitting Devices Based on CdSe/Zn1-xCdx Core/Shell Heterostructured Quantum Dots", Advanced Materials, Volume 26, Issue 47, 7921-8064, (2014)

[8] DeMeo, D., Sonkusale, S., MacNaughton, S., "Nanowires-Implementations and Applications." InTech Europe: Rijeka, Croatia (2011).

[9] DeMeo, D., Sonkusale, S., MacNaughton, S., "Electrodeposited Copper Oxide and Zinc Oxide Core-Shell Nanowire Photovoltaic Cells" Nanowires: Implementations and Applications, (2011)

[10] Vandervelde, T. E., Krishna, S., "Progress and Prospects for Quantum Dots in a Well Infrared Photodetectors", Journal of Nanoscience and Nanotechnology, Volume 10, Number 3, March 2010, pp. 1450-1460 (2010)

[11] Shao, Jiayi; Vandervelde, T. E., Barve, A., Jang, W.Y., Stintz, A., Krishna, S., "Enhanced normal incidence photocurrent in quantum dot infrared photodetectors", J. Vac. Sci. Technol. B, Volume 29, Issue 3, 03C123 (2011)

[12] Guo, S., Gustafsson, G., Hagel, O.J., Arwin, H., "Determination of Refractive Index and Thickness of Thick Transparent Films by Variable-Angle Spectroscopic Ellipsometry: Application to Benzocyclobutene Films.", Applied Optics, vol. 35, no. 10, 1693–1699 (1996)

[13] Kayaku Advanced Materials, Inc. (2019). PMMA Data Sheet, Retrieved from https://kayakuam.com/wp-content/uploads/2019/09/PMMA_Data_Sheet.pdf

[14] Woollam, J.A., Johs, B.D., Herzinger, C.M., Hilfiker, J.N., Synowicki, R.A, Bungay, C.L., " Overview of variable-angle spectroscopic ellipsometry (VASE): I. Basic theory and typical applications.", Proceedings of SPIE - The International Society for Optical Engineering, 10294, 3-28 (1999)

[15] Erman, M., Theeten, J.B., Chambon, P., Kelso, S. M., and Aspnes, D. E., "Optical properties and damage analysis of GaAs single crystals partly amorphized by ion implantation," J. Appl. Phys., Vol. 56, 2664-2671 (1984).

[16] C. M. Herzinger, B. Johs, W. A. McGahan, J. A. Woolam and W. Paulson, J. Appl. Phys., 83, 3323-3336 (1998)

[17] Guo, H., Zhang, F., Wu, G.S., Sun, F., Pu, S., Mai, X., Qi, G., "Multi-wavelength optical storage of diarylethene PMMA film", Optical Materials 22 (2003) 269-274

[18] G. E. Jellison Jr., in Handbook of Ellipsometry, edited by H. G. Tompkins and E. A. Irene (William Andrew Publishing, Norwich, NY, 2005), Pg. 261.

[19] Ke, D., Wathuthanthri, I., Liu, Y., Kang, Y.T., Choi, C.H., "Fabrication of Polymer Nanowires via Maskless O2 Plasma Etching." Nanotechnology, vol. 25, no. 16, 165301, (2014)

[20] Kondyurin, A., Bilek, M., “Etching and structure changes in PMMA coating under argon plasma immersion ion implantation” Nuclear Instruments and Methods in Physics Research Section B: Beam Interactions with Materials and Atoms, 269(11), 1361-1369 (2011)